a SHED-derived condition medium (SHED-CM) in a rat model of cerebral ischemia.

Materials and Methods

SHED harvest from deciduous teeth

Human dental pulp tissues were obtained from clinically healthy, extracted deciduous teeth from eight patients. The ethics committee of the Nagoya University approved the experimental protocols. SHED were isolated and cultured as previously described.[12,13] Briefly, the pulp was removed gently and digested for 1 h at 37°C in a solution containing 3 mg/mL collagenase type I and 4 mg/mL dispase. After filtration through 70-μm cell strainers (Falcon; BD Labware), the cells were cultured at 37°C under 5% CO_2 in the Dulbecco's modified Eagle's medium (DMEM; Gibco) containing 20% mesenchymal cell growth supplement (Lonza, Inc.) and antibiotics (100 U/mL penicillin, 100 mg/mL streptomycin, and 0.25 mg/mL amphotericin B; Gibco). After primary culture, the cells were subcultured at $\sim 1 \times 10^4$ cells/cm^2 and used in the experiments after three to five passages.

Preparation of SHED-CM and BMMSC-CM

SHED and BMMSCs (Lonza, Inc.) (4×10^5 cells) were cultured in a serum-free DMEM. Conditioned media of SHED and BMMSCs were collected after 48 h of culture and centrifuged at 1500 rpm for 5 min. The supernatants were recentrifuged at 3000 rpm for 3 min followed by collection of the second supernatants, named SHED-CM and BMMSC-CM, respectively.

Cerebral ischemia model

All the animal experiments were approved by the Institutional Animal Care and Use Committee (Nagoya University). Adult male Sprague-Dawley rats (Japan SLC, Inc.) weighing 350–400 g were used in the experiments. Animals were anesthetized initially with 5% isoflurane (Abbott Laboratories) and were maintained under anesthesia with 1.5% isoflurane in a mixture of 70% N_2O and 30% O_2. The rectal temperature was maintained at 37°C ± 0.5°C on a heating pad. Focal cerebral ischemia was induced by permanent MCAO (pMCAO) (Fig. 1A).[14] A 4-0 monofilament nylon suture (Shirakawa) with the tip rounded by flame heating and coated with silicone (KE-200; Shin-Etsu Chemical) was advanced from the external carotid artery into the internal carotid artery until it blocked the origin of the MCA. Regional cerebral blood flow in the MCA territory was measured after occlusion using a laser Doppler flowmeter (Omega FLO-N1; Omega Wave, Inc.). The response was considered positive and included only if the reduction in the regional cerebral blood flow was >70%.

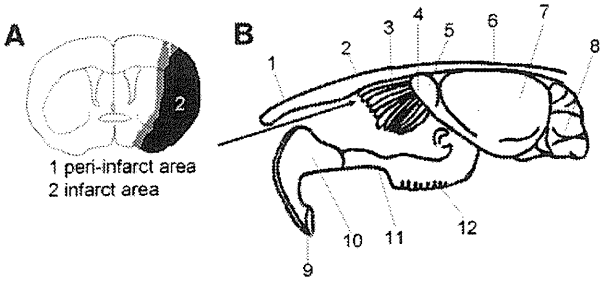

FIG. 1. **(A)** The peri-infarct area. Peri-infarct area (gray) and infarct core (black). **(B)** Anatomy around the olfactory bulb. 1: nasal bone. 2: forehead bone. 3: ethmoid bone. 4: olfactory nerve area. 5: olfactory bulb. 6: forehead bone. 7: cerebrum. 8: cerebellum. 9: incisor teeth. 10: incisive bone. 11: maxilla bone. 12: molar teeth. The arrow displays the passage of nasal administration.

Intranasal administration of the conditioned media and DMEM

Seventy-two hours after pMCAO (day 3), the rats were anesthetized again with 1.5% isoflurane in a mixture of 70% N_2O and 30% O_2. The animals were divided randomly into three groups: the SHED-CM group ($n=7$, three sacrificed on day 6 and four on day 16), the BMMSC-CM group ($n=3$, three sacrificed on day 16), and the DMEM group ($n=7$, three sacrificed on day 6 and four on day 16). The rats were placed on their backs with their necks elevated by a 4 × 4-cm roll of gauze. A total of 100 μL of SHED-CM, BMMSC-CM, and DMEM was administered to each rat via the olfactory pathway using a Hamilton microsyringe (Fig. 1B). The preparations were administered in aliquots of 10 μL at a time and alternated nostril, with an interval of 2 min between each administration. During these procedures, the mouth and opposite nostril were closed. Intranasal administration was performed everyday from days 3 to 15.

Evaluation of motor disability

The rats were blindly examined on days 1, 3, 6, 9, 12, and 15 using a standardized motor disability scale with slight modifications.[15] They scored 1 point for each of the following parameters: flexion of the forelimb contralateral to the stroke side when hung instantly by the tail, extension of the hind limb contralateral to the stroke side when pulled from a table, and rotation to the paretic side against resistance. In addition, 1 point was scored for circling motions to the paretic side when trying to walk, 1 point for failure to walk out of a 50-cm-diameter circle within 10 s, 2 points for failure to leave the circle within 20 s, and 3 points for inability to exit the circle within 60 s. In addition, 1 point each was scored for inability of the rat to extend the paretic forepaw when pushed against the table from above, laterally, and sideways. The motor disability scale was performed 3 times in each animal at each time point.

Assessment of infarct volume

The cryosections obtained from samples on day 16 were stained with hematoxylin and eosin.[16] ImageJ (National Institutes of Health) was used to determine each infarct area in 12 coronal sections (20-μm thick) at 1.00-mm intervals. The entire infarction area was covered by these 12 coronal sections. Regional infarct volumes were calculated by summing the infarct areas and multiplying them by the distance between sections (1.00 mm), followed by remediation for brain edema.[17]

Immunohistochemistry

On day 16 after the injection, the rats were perfused transcardially with a 4% paraformaldehyde solution (Nakarai

Tesque). Their brains were removed, postfixed in paraformaldehyde, and immersed in 30% sucrose solution the following day. Coronal sections (20-μm thick) were then prepared using a cryostat. For immunohistochemistry, the sections were preincubated for 2 h at room temperature (RT) in a blocking solution (Dulbecco's phosphate-buffered saline [PBS] containing 5% normal serum of the species in which the secondary antibody was raised) and incubated for 1 h at RT with diluted primary antibodies. The primary antibodies were as follows: marker of NPC, rabbit anti-doublecortin (anti-DCX; 1:50; Abcam, Inc.), neuronal markers, rabbit anti-neurofilament H (anti-NF; 1:200; Chemicon), mouse anti-neuronal nuclei (anti-NeuN; 1:500; Chemicon), endothelial cell marker, and mouse anti-rat endothelial cell antigen (anti-RECA1; 1:50; Monosan). After washing, the sections were incubated for 1 h at RT with secondary antibodies (NF/DCX, donkey anti-rabbit IgG FITC [1:400; Jackson Immuno-Research], and NeuN/RECA1, goat anti-mouse IgG FITC [1:200; MP Biomedicals, LLC]) and counterstained with 4', 6-diamidino-2-phenylindole (DAPI; Cell Biolabs, Inc.) for sections of DCX, NeuN and RECA1.

The adjacent sections were used as negative controls. In the control sections, all the procedures were performed in a similar manner, with the exception that the primary antibodies were omitted. To identify migration of NPC from the SVZ, we examined anti-DCX-stained cryosections in the SHED-CM and DMEM groups on days 6 and 16 by fluorescence microscopy (BZ-9000; Keyence).

Statistical analyses of cell density

The density of NPC, neurons, and endothelial cells in the peri-infarct (Fig. 1A) area of the SHED-CM and DMEM groups was determined. In these two groups ($n=3$), five sections cut at 100-μm intervals were stained with DCX, NeuN, or RECA1. The microscopic images were scanned, and five typical frames (0.49 mm^2) were measured for each section. Therefore, on an average, 75 frames were determined for each group. The positive-stained area relative to the total area (7.41 mm^2) was statistically analyzed using the software Dynamic cell count (Keyence) and ImageJ.

Statistical analyses

Data are expressed as means ± SD. p values were calculated using the unpaired Student's t test.

Results

Evaluation of motor function

The three groups (SHED-CM, BMMSC-CM, and DMEM) displayed almost the same high score for motor function in the early stages, as shown in Figure 2 (day 1: 8.5 ± 0.58 and 8.33 ± 0.58; 8.75 ± 0.96; day 3: 8.25 ± 0.5, 8.00 ± 1.0, and 8.50 ± 0.6). Differences in the score appeared gradually between the three groups during the middle stage (day 6: 6.75 ± 0.5, 7.33 ± 0.58, 7.80 ± 1.0; day 9: 5.75 ± 0.5, 7.00 ± 1.0, 7.50 ± 1.29). On days 12 and 15, progressive improvement in motor disability became significant in the SHED-CM group compared with that in the DMEM group (day 12: 5.25 ± 0.96, 6.77 ± 0.58, 7.50 ± 1.29; day 15: 4.0 ± 0.81, 6.33 ± 0.58, 7.25 ± 1.26). On day 15, progressive improvement in motor disability became significant in the SHED-CM group compared with that in the BMMSC-CM group.

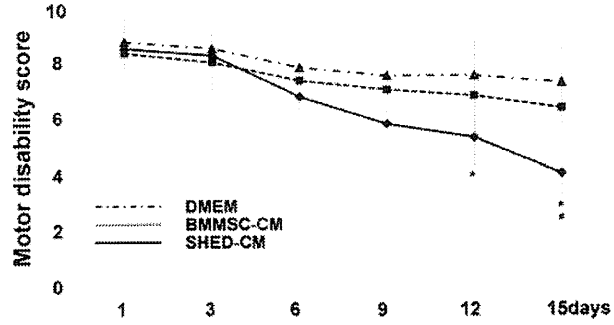

FIG. 2. Motor disability test following intranasal administration of stem cells from human exfoliated deciduous tooth (SHED)-derived conditioned medium (SHED-CM), bone marrow mesenchymal stem cell (BMMSC)-derived conditioned medium (BMMSC-CM), and Dulbecco's modified Eagle's medium (DMEM) on days 1, 3, 6, 9, 12, and 15. Data are expressed as means ± SD of 3 determinations. $^{*}p<0.05$, versus DMEM. $^{\#}p<0.05$ versus BMMSC-CM. Student's t-test.

Reduction in infarct volume

As shown in Figure 3, there was a significant decrease in the infarct volume on day 16 in the SHED-CM group (day 16, 52.20 ± 14.7 mm^3, $n=3$) compared with the BMMSC-CM (day 16, 113.62 ± 10.77 mm^3, $n=3$) and DMEM groups (day 16, 147.43 ± 5.50 mm^3, $n=3$). These results suggest that SHED-CM promote regeneration.

SHED-CM outcome

In the immunohistochemistry experiments, the SHED-CM group had more positive signals for DCX (Fig. 4A), NF (Fig. 4C), NeuN (Fig. 4E), and RECA1 (Fig. 4G) in the peri-infarct

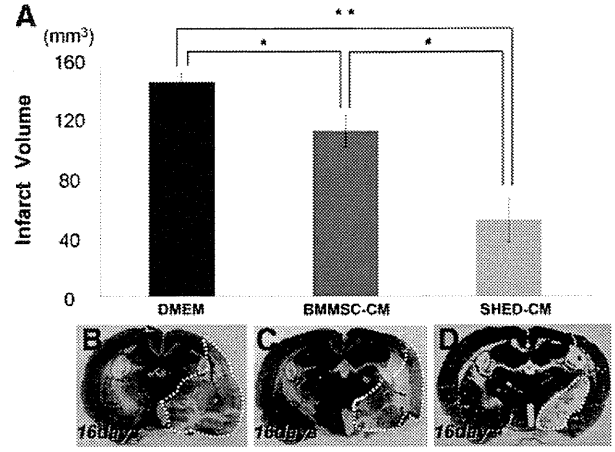

FIG. 3. Reduction in the infarct volume 16 days after the injection of SHED-CM, BMMSC-CM, and DMEM **(A)**. Infarct area on day 16 after nasal injection (**B**:DMEM, **C**:BMMSC-CM, and **D**:SHED-CM). Data are expressed as means ± SD of 3 determinations **(A)**. $^{*}p<0.05$, $^{**}p<0.01$, versus DMEM, $^{\#}p<0.05$, versus BMMSC-CM. Student's t-test.

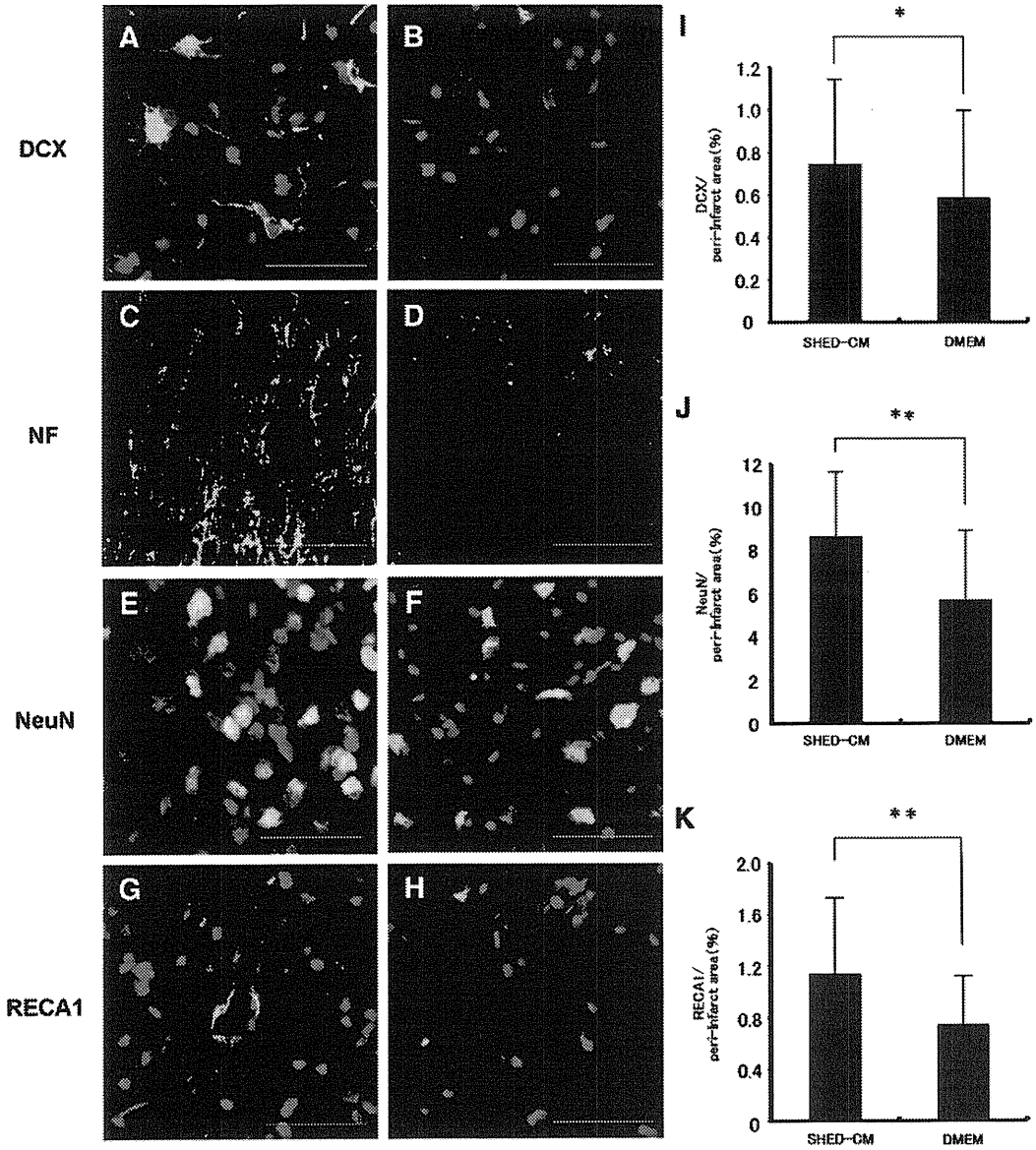

FIG. 4. Doublecortin (DCX)-positive cells **(A, B)**, neurofilament H (NF)-positive cells **(C, D)**, neuronal nucleus (NeuN)-positive cells **(E, F)**, and rat endothelial cell antigen (RECA1)-positive cells **(G, H)**. SHED-CM group **(A, C, E, G)** on day 16. DMEM group **(B, D, F, H)** on day 16. Bar = 50 μm **(A–H)**. Cell nuclei were counterstained with DAPI. Statistical analyses of density of DCX **(I)**, NeuN **(J)**, and RECA1 **(K)** on day 16. $*p < 0.05$, $**p < 0.001$, Student's *t*-test. Each point is expressed as the mean ± SD of 75 determinations. Color images available online at www.liebertpub.com/tea

area compared with the DMEM group (Fig. 4B, D, F, H). Cell nuclei were labeled with DAPI (blue). There was a 1.27-fold increase in DCX-positive cells (Fig. 4I), 1.52-fold increase in NeuN-positive cells (Fig. 4J), and 1.53-fold increase in RECA1-positive cells (Fig. 4K) on day 16 in the SHED-CM group than in the DMEM group. The migration of NPC with DCX from the SVZ to the peri-infarct area was observed on days 6 (Fig. 5A) and 16 (Fig. 5C). The migration on day 6 was most prominent (Fig. 5A). These results suggest that SHED-CM also promote neurogenesis and angiogenesis after cerebral ischemia.

Discussion

We reported the characteristics of SHED compared with those of DPSC and BMMSCs. The results indicated that SHED possessed high proliferation ability and were enriched with the extracellular matrix, suggesting that they may be a useful source for stem cell-based therapy. In addition, using microarray analysis, we showed that SHED had higher expression levels of several growth factors, such as fibroblast growth factor, transforming growth factor, connective tissue growth factor, nerve growth factor, and bone morphogenetic

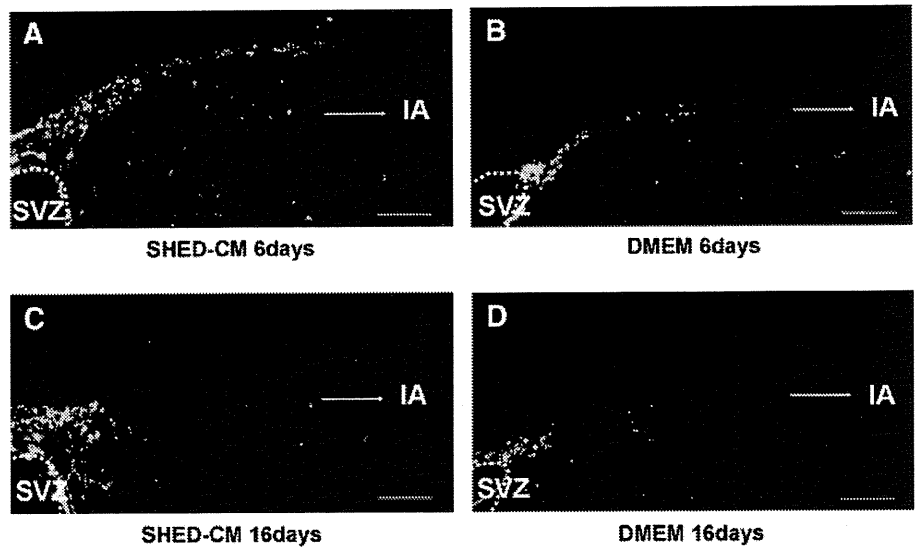

FIG. 5. Migration of neuronal progenitor cells (NPC) from the SVZ to the peri-infarct area on days 6 **(A, B)** and 16 **(C, D)**. SHED-CM intranasal group **(A, C)**. DMEM intranasal group **(B, D)**. Bar = 100 μm **(A–D)**. IA = infarct area. Color images available online at www.liebertpub.com/tea

protein.[5] Taken together, these findings indicate that SHED are a more potentially useful source of stem cells for cell therapy than DPSC and BMMSCs.

However, cell therapy is always associated with problems, such as canceration,[18] immune rejection, and ethics issues. Therefore, it is necessary to find alternative treatments. Studies in recent years have resulted in the recognition of a paracrine function in factors, and have suggested that stem cell transplantation may also be regarded as cell-based cytokine therapy.[7,8] Accordingly, we investigated two steps for developing a new treatment for cerebral ischemia.

In the first step, we used SHED-CM as a new source for the treatment of cerebral ischemia. We have previously reported that needle administration of DPSC induced the recovery of motor disability and reduction in the infarct volume, proliferation of presumptive progeny in the SVZ, migration to the infarct, and differentiation into the appropriate neurons in a rat model of stroke.[7] As several growth factors involved in neural regeneration are secreted from DPSC, we hypothesized that SHED-CM may improve the recovery of motor disability and reduce the infarct volume in the present study.

Moreover, we showed that the SHED-CM group significantly improved motor function and infarct volume compared with the BMMSC group (Figs. 2 and 3A).

Furthermore, the SHED-CM group had more positive signals for DCX, NF, NeuN, and RECA1 in the peri-infarct area (Fig. 1A) compared with the DMEM group (Fig. 4A–K). Migration of NPC with DCX from the SVZ to the peri-infarct area was observed on days 6 and 16, with the migration being the most prominent on day 6 in the SHED-CM group (Fig. 5A–D).

Brain injury is known to upregulate nestin expression.[19] Nestin-positive, pluripotent NPC mature into neuroblasts that are positive for DCX.[20] We found an increase in the DCX-positive population in pMCAO-injured animals treated with SHED-CM. Our results suggested that SHED-CM may trigger proliferation of NPC, and given the significant improvement in behavioral response, it is likely that these progenitor cells participate in the generation of new neurons.

In the second step, we investigated the intranasal administration of SHED-CM. Using this administration, therapeutic molecules traverse the BBB through the olfactory pathway and the less-studied trigeminal neural pathway.[21] An important advantage of intranasal administration is that it is less invasive, with the factors being delivered directly to the brain.

Recently, it was reported that VEGF as a growth factor can bypass the BBB to reach multiple sites within the brain ~30 min after the start of intranasal administration, and that intranasal administration may result in decreased systemic side effects because of decreased concentration in blood and peripheral organs.[11] Our results suggested that SHED-CM, including some growth factors, may produce effects similar to those seen with VEGF in a stroke model.

The success of the two investigated steps suggests the possibility of using a shortcut in a clinical setting. Administration of SHED-CM resolves the ethics issues involved with cell therapies, because SHED-CM are not a cell, but a conjugate of many growth factors. As SHED-CM can be stocked, it is possible to use it for the acute stages of stroke, either alone or with readily available treatments, such as recombinant tissue plasminogen activator, anticoagulation, and antiplatelet therapy.

This study suggests that intranasal administration of SHED-CM may help in the recovery of acute stroke patients in future. In conclusion, regeneration therapy using SHED-CM is very safe with no associated problems; therefore, it is a potential candidate for the innovative treatment of cerebral ischemia.

Acknowledgments

We thank Mrs. Mami Naruse for her assistance. This work was supported by funds from the Collaborative Development of Innovative Seeds, Potentiality Verification Stage from Japan Science and Technology Agency, and a Grant-in-Aid for Scientific Research from the Ministry of Education, Science, Sports and Culture, Japan, #22890082 (M.S.).

Disclosure Statement

No competing financial interests exist.

References

1. Donnan G.A., Fisher, M., Macleod, M., and Davis, S.M. Stroke. Lancet **371,** 1612, 2008.
2. Honmou, O., Houkin, K., Matsunaga, T., Niitsu, Y., Ishiai, S., Onodera, R., Waxman, S.G., and Kocsis, J.D. Intravenous administration of auto serum-expanded autologous mesenchymal stem cells in stroke. Brain **134,** 1790, 2011.
3. Bang, O.Y., Lee, J.S., Lee, P.H., and Lee, G. Autologous mesenchymal stem cell transplantation in stroke patients. Ann Neurol **57,** 874, 2005.
4. Kern, S., Eichler, H., Stoeve, J., Klüter, H., and Bieback, K. Comparative analysis of mesenchymal stem cells from bone marrow, umbilical cord blood, or adipose tissue. Stem Cells **24,** 1294, 2006.
5. Nakamura, S., Yamada, Y., Katagiri, W., Sugito, T., Ito, K., and Ueda, M. Stem cell proliferation pathways comparison between human exfoliated deciduous teeth and dental pulp stem cells by gene expression profile from promising dental pulp. J Endod **35,** 1536, 2009.
6. Pierdomenico, L., Bonsi, L., Calvitti, M., Rondelli, D., Arpinati, M., Chirumbolo, G., Becchetti, E., Marchionni, C., Alviano, F., Fossati, V., Staffolani, N., Franchina, M., Grossi, A., and Bagnara, G.P. Multipotent mesenchymal stem cells with immunosuppressive activity can be easily isolated from dental pulp. Transplantation **80,** 836, 2005.
7. Sugiyama, M., Iohara, K., Wakita, H., Hattori, H., Ueda, M., Matsushita, K., and Nakashima, M. Dental pulp-derived CD31{/CD146{ side population stem/progenitor cells enhance recovery of focal cerebral ischemia in rats. Tissue Eng Part A **17,** 1303, 2011.
8. Nicaise, C., Mitrecic, D., and Pochet, R. Brain and spinal cord affected by amyotrophic lateral sclerosis induce differential growth factors expression in rat mesenchymal and neural stem cells. Neuropathol Appl Neurobiol **37,**179, 2011.
9. Illum, L. Transport of drugs from the nasal cavity to the central nervous system. Eur J Pharm Sci **11,** 1, 2000.
10. Thorne, R.G. and Frey, W.H. 2nd. Delivery of neurotrophic factors to the central nervous system: pharmacokinetic considerations. Clin Pharmacokinet **40,** 907, 2001.
11. Yang, J.P., Liu, H.J., Wang, Z.L., Cheng, S.M., Cheng, X., Xu, G.L., and Liu, X.F. The dose-effectiveness of intranasal VEGF in treatment of experimental stroke. Neurosci Lett **461,** 212, 2009.
12. Gronthos, S., Mankai, M., Brahim, J., Robey, P.G., and Shi, S. Postnatal human dental pulp stem cells (DPSC) *in vitro* and *in vivo*. Proc Natl Acad Sci U S A **97,** 13625, 2000.
13. Miura, M., Gronthos, S., Zhao, M., Lu, B., Fisher, L.W., Robey, P.G., and Shi, S. SHED: stem cells from human exfoliated deciduous teeth. Proc Natl Acad Sci U S A **100,** 5807, 2003.
14. Longa, E.Z., Weinstein, P.R., Carlson, S., and Cummins, R. Reversible middle cerebral artery occlusion without craniectomy in rats. Stroke **20,** 84, 1989.
15. Leker, R.R., Gai, N., Mechoulam, R., and Ovadia, H. Drug-induced hypothermia reduces ischemic damage: effects of the cannabinoid HU-210. Stroke **34,** 2000, 2003.
16. Ginsberg, M.D. Adventures in the pathophysiology of brain ischemia: penumbra, gene expression, neuroprotection: the 2002 Thomas Willis Lecture. Stroke **34,** 214, 2003.
17. Leach, M.J, Swan, J.H, Eisenthal, D., Dopson, M., and Nobbs, M. BW619C89, a glutamate release inhibitor, protects against focal cerebral ischemic damage. Stroke **24,** 1063, 1993.
18. Ooi, A.T., Mah, V., Nickerson, D.W., Gilbert, J.L., Ha, V.L., Hegab, A.E., Horvath, S., Alavi, M., Maresh, E.L., Chia, D., Gower, A.C., Lenburg, M.E., Spira, A., Solis, L.M., Wistuba, I.I., Walser, T.C., Wallace, W.D., Dubinett, S.M., Goodglick, L., and Gomperts, B.N. Presence of a putative tumor-initiating progenitor cell population predicts poor prognosis in smokers with non-small cell lung cancer. Cancer Res **70,** 6639, 2010.
19. Frisén, J., Johansson, C.B., Török, C., Risling, M., and Lendahl, U. Rapid, widespread, and longlasting induction of nestin contributes to the generation of glial scar tissue after CNS injury. J Cell Biol **131,** 453, 1995.
20. Itoh, T., Satou, T., Takemori, K., Hashimoto, S., and Ito, H. Neural stem cells and new neurons in the cerebral cortex of stroke-prone spontaneously hypertensive rats after stroke. J Mol Neurosci **41,** 55, 2010.
21. Thorne, R.G., Pronk, G.J., Padmanabhan, V., and Frey, W.H. 2nd. Delivery of insulin-like growth factor-I to the rat brain and spinal cord along olfactory and trigeminal pathways following intranasal administration. Neuroscience **127,** 481, 2004.

Address correspondence to:
Hisashi Hattori, Ph.D.
Department of Oral and Maxillofacial Surgery
Laboratory Medicine
Nagoya University Graduate School of Medicine
65 Tsurumai-cho
Shouwa-ku
Nagoya 466-8550
Japan

E-mail: hattori6@med.nagoya-u.ac.jp

Received: July 8, 2011
Accepted: July 9, 2012
Online Publication Date: October 9, 2012

Biochemical and Biophysical Research Communications 430 (2013) 763–768

Contents lists available at SciVerse ScienceDirect

Biochemical and Biophysical Research Communications

journal homepage: www.elsevier.com/locate/ybbrc

Novel application of stem cell-derived factors for periodontal regeneration

Takeharu Inukai, Wataru Katagiri *, Ryoko Yoshimi, Masashi Osugi, Takamasa Kawai, Hideharu Hibi, Minoru Ueda

Department of Oral and Maxillofacial Surgery, Nagoya University Graduate School of Medicine, Japan

ARTICLE INFO

Article history:
Received 7 November 2012
Available online 1 December 2012

Keywords:
Cytokine
Periodontal regeneration
Mesenchymal stem cell
Conditioned medium
Paracrine

ABSTRACT

The effect of conditioned medium from cultured mesenchymal stem cells (MSC-CM) on periodontal regeneration was evaluated. *In vitro*, MSC-CM stimulated migration and proliferation of dog MSCs (dMSCs) and dog periodontal ligament cells (dPDLCs). Cytokines such as insulin-like growth factor, vascular endothelial growth factor, transforming growth factor-β1, and hepatocyte growth factor were detected in MSC-CM. *In vivo*, one-wall critical-size, intrabony periodontal defects were surgically created in the mandible of dogs. Dogs with these defects were divided into three groups that received MSC-CM, PBS, or no implants. Absorbable atelo-collagen sponges (TERUPLUG®) were used as a scaffold material. Based on radiographic and histological observation 4 weeks after transplantation, the defect sites in the MSC-CM group displayed significantly greater alveolar bone and cementum regeneration than the other groups. These findings suggest that MSC-CM enhanced periodontal regeneration due to multiple cytokines contained in MSC-CM.

1. Introduction

Periodontitis is an infection or inflammation that causes destruction of the periodontal tissues, including gingiva, root cementum, alveolar bone, and the periodontal ligament (PDL). A goal of periodontal regenerative therapy is to return the tissues to their original condition and restore the form and function of the lost structures [1].

Many experimental and clinical studies about periodontal tissue engineering and regenerative medicine have been published. Historically, various regenerative methods and materials, including guided tissue regeneration [2,3], enamel matrix protein derivative (Emdogain®) [4], and osteoinductive agents and biomaterials, have been used in clinical practice for periodontal regeneration [5,6]. Cell therapy is expected to become the next-generation method. The concepts of tissue engineering and regenerative medicine involve the regeneration of tissues using a combination of cells, scaffolds, and signaling molecules [7]. Mesenchymal stem cells (MSCs) are well known to secrete a variety of growth factors and cytokines [8]. Recent studies have indicated that the paracrine effects of the growth factors and cytokines secreted from implanted MSCs may promote tissue regeneration *in vivo* [9,10]. Conditioned medium from cultured mesenchymal stem cells (MSC-CM) has been reported to have multiple positive functions in tissue regeneration [10,11]. We previously reported that bone marrow-derived MSC-CM has a very high potential for bone regeneration that is mediated by the cooperative effects of cytokines such as insulin-like growth factor-1 (IGF-1), vascular endothelial growth factor (VEGF), and transforming growth factor-β1 (TGF-β1), which regulate several events of osteogenesis, including angiogenesis, cell migration, proliferation, and osteoblast differentiation [12]. Based on these findings, we hypothesized that transplantation of MSC-CM may play an important role in periodontal tissue regeneration and overcome limitations of existing therapies. The purpose of this study was to evaluate the effect of MSC-CM on periodontal regeneration.

2. Materials and methods

2.1. Cell isolation, cultivation, and preparation of MSC-CM

Dog MSCs (dMSCs) and dog periodontal ligament cells (dPDLCs) were isolated from five hybrid dogs (age 18–36 months, weight 15–25 kg) and expanded in accordance with published techniques

Abbreviations: MSC, mesenchymal stem cells; dPDLCs, dog periodontal ligament cells; IGF-1, insulin-like growth factor-1; VEGF, vascular endothelial growth factor; TGF-β1, transforming growth factor-β1; HGF, hepatocyte growth factor; FGF-2, fibroblast growth factor-2; PDGF-BB, platelet-derived growth factor-BB; BMP-2, bone morphogenetic protein-2; SDF-1, stromal cell-derived factor-1; PDL, periodontal ligament; FBS, fetal bovine serum; ELISA, enzyme-linked immunosorbent assay.

* Corresponding author. Address: Department of Oral and Maxillofacial Surgery, Nagoya University Graduate School of Medicine, 65 Tsurumai-cho, Showa-ku, Nagoya, Aichi 466-8550, Japan. Fax: +81 52 744 2352.

E-mail addresses: t-inukai@med.nagoya-u.ac.jp (T. Inukai), w-kat@med.nagoya-u.ac.jp (W. Katagiri), lianzi@med.nagoya-u.ac.jp (R. Yoshimi), masashi@med.nagoya-u.ac.jp (M. Osugi), takamasa@med.nagoya-u.ac.jp (T. Kawai), hibihi@med.nagoya-u.ac.jp (H. Hibi), mueda@med.nagoya-u.ac.jp (M. Ueda).

0006-291X/$ - see front matter © 2012 Elsevier Inc. All rights reserved.
http://dx.doi.org/10.1016/j.bbrc.2012.11.074

[13,14]. Human MSCs (hMSCs) were purchased from Lonza and cultured according to the manufacturer's instructions. All cells in this experiment were cultured at 37 °C with 5% CO_2 and 95% air in a humidified incubator. dMSCs (2nd-4th passage), dPDLCs (2nd-3th passage), and hMSCs (3rd-9th passage) were used for the experiments.

At approximately 70% confluency, the conditioned medium of hMSCs was refreshed with serum-free Dulbecco's Modified Eagle Medium (DMEM) and cultured for an additional 48 h. MSC-CM was collected and stored at 4 °C or −80 °C before use in the following experiments.

2.2. Migration and proliferation of dMSCs and dPDLCs

Transwell dishes with 8.0-μm pore filters (BD BioCoat™ Control Inserts; Becton Dickinson and Co., Franklin Lakes, NJ) were used for the migration assays. dMSCs (5×10^5 cells/cm^2) or dPDLCs (5×10^5 cells/cm^2) were seeded into the upper chamber, and MSC-CM was added to the lower chamber. Cell migration was observed in the presence of 30% FBS or serum-free DMEM, which served as positive and negative controls, respectively. After 48 h of culture, the upper side of the filters was carefully rinsed with PBS, and the remaining cells on the upper surface of the filters were mechanically removed with a cotton-wool swab. Transwell filters were stained with hematoxylin, cut with a scalpel, and mounted onto glass slides, with the lower surface facing upward. The proliferation rate of approximately 70% confluent dMSCs and dPDLCs was assessed with bromodeoxyuridine (BrdU) incorporation for 24 h, using a Zymed BrdU staining kit (Invitrogen, Carlsbad, CA) according to the manufacturer's instructions. Both the number of migrated dMSCs and dPDLCs and the percentages of BrdU-positive cells were counted in five randomly selected fields using a light microscope (CK40; Olympus, Tokyo, Japan) at 200× magnification.

2.3. Enzyme-linked immunosorbent assay (ELISA)

To evaluate the cytokines in MSC-CM, ELISA for IGF-1, VEGF, fibroblast growth factor-2 (FGF-2), TGF-β1, hepatocyte growth factor (HGF), platelet-derived growth factor-BB (PDGF-BB), bone morphogenetic protein-2 (BMP-2), and stromal cell-derived factor-1 (SDF-1) in MSC-CM were performed. The concentrations of these factors were measured using a Human Quantikine ELISA kit (R&D Systems, Minneapolis, MN) according to the manufacturer's instructions.

2.4. Dog one-wall intrabony defect model

All animal experiments were approved by the Nagoya University animal experiment committee. After a period of acclimatization of 30 days, five hybrid dogs were operated on under general anesthesia by intravenous injection of pentobarbital (Somnopentyl®; Kyoritsu Seiyaku, Tokyo, Japan) (20 mg/kg body weight), and under local anesthesia with 2% lidocaine (with 1:80,000 epinephrine, ORA® Inj. Dental Cartridge; Showa Yakuhin Kako, Tokyo, Japan). Before the experimental surgery, the mandibular first and third or fourth premolars were extracted, and the extraction sites were allowed to heal for 8 weeks. For the experimental surgery, buccal and lingual mucoperiosteal flaps were elevated, and critical-size, box-type, one-wall intrabony defects (width, 4 mm; height, 5 mm) were created at the distal aspect of the second, and the mesial aspect of the fourth premolars in the right and left jaw quadrants [15]. Following root planing to remove the root cementum, a reference notch indicating a 5-mm distance from the cement-enamel junction to the bottom of the defect was made with a burr into the root surface at the base of the defects. With no differences in bone regeneration in the various grafted areas in terms of bone healing, two defects were created and implanted with two materials at random sites. An absorbable atelo-collagen sponge (TERUPLUG®; OLYMPUS TERUMO BIOMATERIALS, Tokyo, Japan) was used as a scaffold and contained 300 μl MSC-CM or PBS. The dogs with defects were randomly divided into three groups ($n = 6$ each) and implanted with graft materials: MSC-CM plus scaffold, PBS plus scaffold, or no implant/scaffold. The mucogingival flaps were advanced, adapted, and completely closed. Post-surgical management involved antibiotics (Azithromycin, 250 mg; Pfizer, Tokyo, Japan) daily for 3 days, a soft diet, and topical application of 2% chlorhexidine (Hibitane concentrate; Dainippon Sumitomo Pharma, Osaka, Japan) twice a week. After 4 weeks, the dogs were given general anesthesia and sacrificed by exsanguination after injection of heparin sodium (400 U/kg).

2.5. Radiographic and histological analyses

Standardized radiographic images of the defect sites were obtained with an X-ray apparatus (Dent navi Hands; Yoshida Co., Ltd., Tokyo, Japan) and dental X-ray films (BW-100; Hanshin Technical Laboratory, Nishinomiya, Japan) immediately, and 4 weeks after, transplantation. Dental X-ray films were placed parallel to the tooth axis, and radiographic images of the defect site were taken in the buccolingual direction. The defect sites were dissected and fixed in 10% neutral-buffered formalin (Wako, Japan) 4 weeks after transplantation. The specimens were decalcified in Plank-Rychro solution (Wako) for 8 weeks, routinely processed into 5-μm-thick paraffin-embedded sections, stained with hematoxylin and eosin, and observed under a light microscope (Olympus). Histometric parameters were quantified using a computer-based image analysis system (ImageJ 1.44; National Institutes of Health). The following parameters were analyzed:

(1) Cementum regeneration height: distance from the root surface notch to the coronal extension of newly formed cementum on the root surface.
(2) Bone regeneration height: distance from the root surface notch to the coronal extension of newly formed bone along the root surface.
(3) Bone regeneration area: area of new alveolar bone formed coronally from the apical extension of the root surface notch.

2.6. Statistical analysis

Summary statistics (mean ± SD) based on animal means for the experimental treatments were calculated using the three central sections from each defect. Statistical differences were evaluated with Tukey's HSD (Honestly Significant Difference) test (IBM SPSS statistics 19). A value of $p < 0.05$ was considered statistically significant.

3. Results

3.1. Effect of MSC-CM on dMSC migration and proliferation

The numbers of migrated dMSCs in DMEM (−), 30% FBS, and MSC-CM were 4.47 ± 3.10, 54.1 ± 13.03, and 43.87 ± 13.03, respectively (Fig. 1A, left). The numbers of migrated dPDLCs in DMEM (−), 30% FBS, and MSC-CM were 4.38 ± 1.19, 40.75 ± 5.70, and 33.0 ± 6.0, respectively (Fig. 1A, right). The percentages of BrdU-positive dMSCs cultured in DMEM (−), 30% FBS, and MSC-CM were 39.41 ± 6.76%, 69.74 ± 4.97%, and 55.31 ± 8.39%, respectively (Fig. 1B, left). The percentages of BrdU-positive dPDLCs cultured in DMEM (−), 30% FBS, and MSC-CM were 30.23 ± 7.99%, 65.49 ± 6.58%, and 61.1 ± 4.69%, respectively (Fig. 1B, right). These

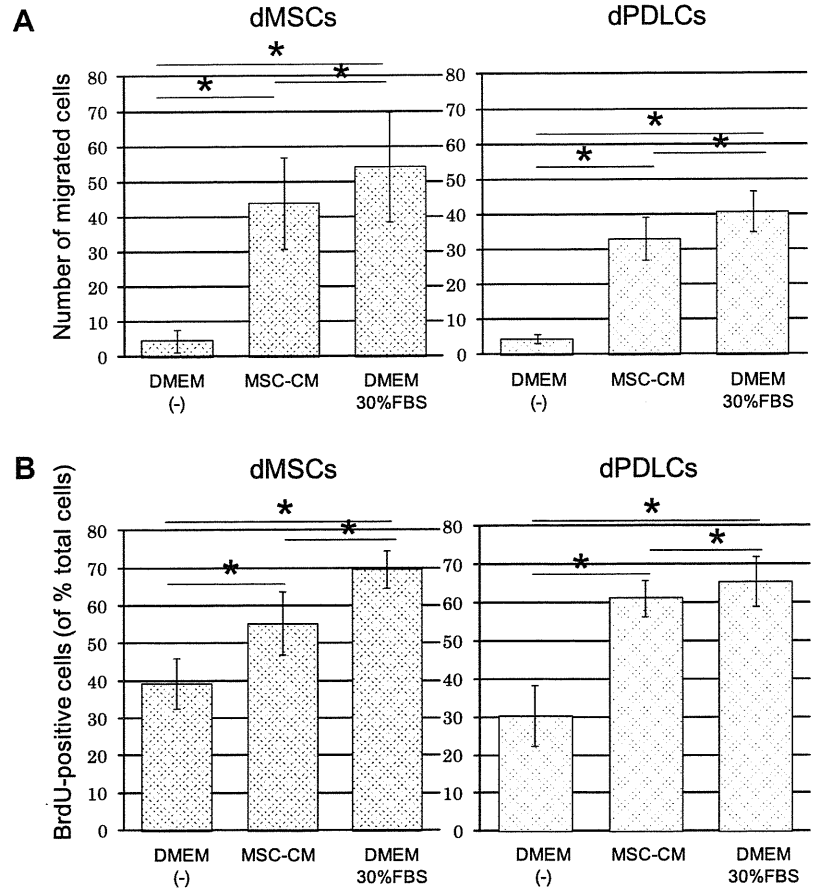

Fig. 1. (A) Transwell migration assay. The migration of dMSCs and dPDLCs cultured in MSC-CM were enhanced compared to that of dMSCs cultured in DMEM (−). (B) BrdU assay. The proliferation of dMSCs and dPDLCs cultured in MSC-CM was also enhanced compared to culturing in DMEM (−). Cells cultured in DMEM + 30%FBS were used as a positive control for both (A) and (B). Asterisks indicate a significant difference between the indicated groups ($p < 0.05$).

differences were statistically significant ($p < 0.05$), indicating that MSC-CM enhanced migration and proliferation of dMSCs and dPDLCs similar to serum-containing medium, compared with serum-free medium.

3.2. Growth factors present in MSC-CM

The concentrations of IGF-1, VEGF, TGF-β1, HGF, FGF-2, PDGF-BB, BMP-2, and SDF-1 in MSC-CM were analyzed using ELISA. These factors were not detected in DMEM (−) or 30% FBS. However, in MSC-CM, the concentrations of IGF-1, VEGF, TGF-β1, and HGF were 1515.6 ± 211.8 pg/ml, 465.8 ± 108.8 pg/ml, 339.8 ± 14.4 pg/ml, and 20.3 ± 7.9 pg/ml, respectively. Other factors were not detected in MSC-CM.

3.3. Radiographic and histological analyses

Clinical healing was generally uneventful. Representative photomicrographs of the experimental sites are shown in Fig. 2. The results from the histometric analysis are shown in Fig. 3. The cementum regeneration height, the bone regeneration height, and the bone regeneration area of the MSC-CM group were 3.01 ± 0.16 mm, 3.19 ± 0.51 mm, and 4.89 ± 1.08 mm^2, respectively. A large amount of new lamellar and woven bone formation was observed in the MSC-CM group. Thick-layered and cellular cementum on the root surface was also frequently observed in the MSC-CM group.

On the other hand, less newly regenerated bone and cementum compared to the MSC-CM group was observed in the PBS group. Dense collagen fibers were observed frequently in the PBS group. Newly regenerated bone and cementum were not apparent in the no implant group. Furthermore, there was minimal inflammatory cell infiltration in the MSC-CM group compared to the other groups.

4. Discussion

To regenerate periodontal tissue destroyed by periodontitis, several events are required, including angiogenesis, cell migration, proliferation, and differentiation into osteoblasts and cementblasts on the dental root and alveolar bone surfaces facing the region of the periodontal tissue defect, followed by regeneration of the alveolar bone and cementum. Historically, periodontal therapies have been developed, including conventional periodontal therapies such as gingival flap surgery that cleans root surfaces and improves periodontal form. Therefore, the disease process is arrested, and periodontal tissues are repaired [3]. Guided tissue regeneration is a surgical procedure that utilizes a barrier membrane that is placed under the gingiva and over the remaining bone to prevent epithelial down-growth and fibroblast trans-growth into the wound space, thereby maintaining a space for true periodontal tissue regeneration [2,3]. Autogenous bone grafting is considered to be an effective method [16], but it requires a wider surgical area. Moreover, tooth-debilitating occurrence of root resorption and ankylosis after grafting of autogenous bone have also been re-

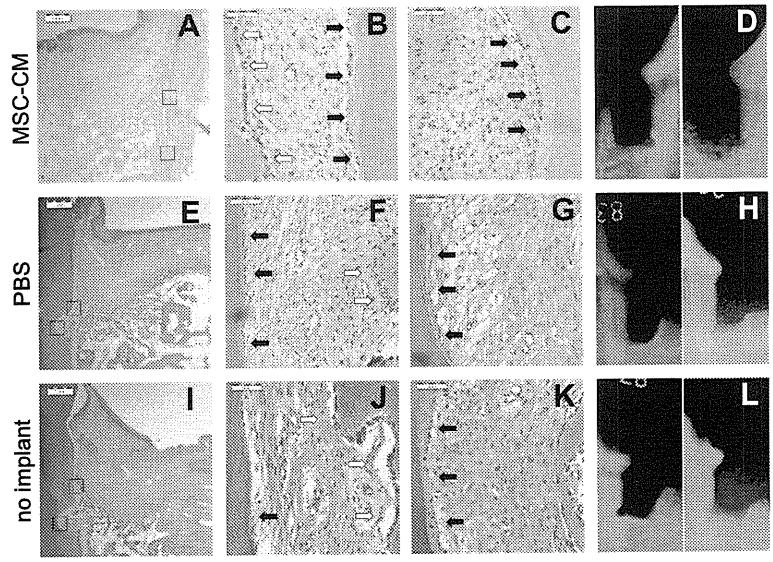

Fig. 2. Representative photomicrographs and radiographic images from sites receiving experimental materials. (A, E and I) overview of periodontal defect site. Original magnification × 12.5, scale bar = 1 mm. (B, C, F, G, J and K) Higher magnification of the boxed areas. Original magnification × 100, scale bar = 50 μm. (D, H and L) Radiographic images were taken at 0 (left) and 4 weeks (right) after surgery. White arrows: osteoblasts. Black arrows: newly regenerated cellular cementum. Photomicrographs: hematoxylin and eosin staining.

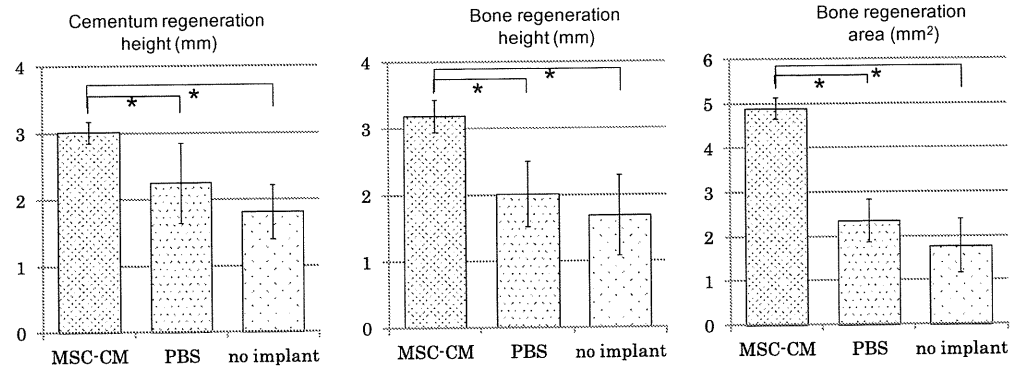

Fig. 3. Histometric analysis of periodontal regeneration following surgical implantation of MSC-CM/TERUPLUG® in dog one-wall intrabony defects (means ± SD in mm or mm²). *Statistical difference ($p < 0.05$), $n = 5$.

ported [17]. Although allografts, xenografts, and osteoinductive biomaterials (beta-tricalcium phosphate, hydroxyapatite) are available, these materials also have poor osteoinductivity and provide a risk of infection and immunological rejection [5,6]. On the other hand, enamel matrix protein derivative (Emdogain®) has shown favorable clinical results for reducing intrabony periodontal defects [4].

Cytokines enhance periodontal regeneration by stimulating the proliferation of mesenchymal cells in the periodontal tissue and differentiation into osteoblasts/cementblasts [18]. PDGF-BB and BMP-2 are already on the market [19]. The efficacy of local application of recombinant human FGF-2 [20] has been investigated in a clinical study. The significant difference in rate of increase in alveolar bone height suggests that FGF-2 therapy can be efficacious in regenerating periodontal tissue. Application of TGF-β [21], BMP-7 [22], brain-derived neurotrophic factor [23], and growth and differentiation factor-5 [24–26] has been reported *in vitro* and *in vivo*. These factors enhance cellular activation of osteogenesis [27]. However, application of a single growth factor has limited bone regeneration ability, and outcomes are not always predictable. In addition, application of these growth factors unfortunately requires superphysiological doses [28] and may induce a severe inflammatory response [29]. Therefore, a combination of several different factors will likely be better for optimizing bone regeneration [30–33].

Recently, many experimental and clinical studies of cell therapies for periodontal regeneration have been conducted. Grafting human cultured periosteum sheets for periodontal defects was reported [34]. We previously used an injectable tissue-engineered bone that is a mixture of hMSCs and platelet-rich plasma as bone graft materials [35]. However, the field is hampered by problems such as the need for large capital investment, expensive cell culture, complicated safety and quality management, and the oncogenic risk of grafted cells.

Implanted cells do not survive for a long time [36–40]. On the other hand, implanted MSCs secrete a variety of cytokines [8], and several cytokines are present in MSC-CM [41]. These findings suggest that the paracrine effects of multiple cytokines secreted from implanted MSCs may promote tissue regeneration [9–11]. We previously reported that MSC-CM has a very high potential for bone regeneration that is mediated by the cooperative effects of cytokines such as IGF-1, VEGF, TGF-β1, and HGF. These cytokines

regulate several events of osteogenesis, including angiogenesis, cell migration, proliferation, and osteoblast differentiation [12]. IGF-1 induces osteoblast proliferation and migration [42,43] and enhances periodontal regeneration by stimulating PDL cells through the PI3K pathway [44]. VEGF is thought to be the main regulator of angiogenesis. VEGF also enhances survival and differentiation of endothelial cells, and as a result, it contributes to osteogenesis [45]. TGF-β1 increases bone formation by recruiting osteoprogenitor cells and stimulating their proliferation and differentiation into osteocytes [46]. TGF-β1 also stimulates PDL regeneration and repair [47] and is expressed during the development of the alveolar bone, PDL, and cementum [48]. HGF is a potent angiogenic molecule, and this activity is mediated primarily through direct actions on vascular endothelial cells [49]. Based on these findings, we predicted that cooperative effects between these cytokines and other unknown factors towards angiogenesis and osteogenesis would mediate periodontal regeneration induced by MSC-CM after endogenous cell mobilization.

TERUPLUG®, which we use as a scaffold, is an absorbable atelocollagen sponge that is highly biocompatible [50]. It is easy to infiltrate MSC-CM into TERUPLUG and adapt it to the bone defect shape. The product is in a sponge block configuration. Also, it serves as a scaffold for osteoblast migration.

Compared with a previous study also using the one-wall intrabony periodontal defect model [23–25], the histological results in the present study at 4 weeks after treatment were equivalent to the results from the other study at 8 weeks after treatment. These results support the hypothesis that MSC-CM enhances periodontal regeneration.

This novel regenerative technique based on a unique concept that utilizes endogenous stem cells without cell transplantation may represent an alternative solution for periodontal regeneration, overcoming the limitations of existing therapies.

Acknowledgments

The authors would like to thank the members of the Department of Oral and Maxillofacial Surgery for their assistance. This work was supported in part by Grants-in-Aid for Scientific Research (Nos. 21791985 and 23592883) from the Ministry of Education, Culture, Sports, and Technology of Japan.

References

[1] D.D. Bosshardt, A. Sculean, Does periodontal tissue regeneration really work?, Periodontology 2000 (51) (2009) 208–219
[2] C.C. Villar, D.L. Cochran, Regeneration of periodontal tissues: guided tissue regeneration, Dent. Clin. North Am. 54 (2010) 73–92.
[3] P. Ratka-Krüger, E. Neukranz, P. Raetzke, Guided tissue regeneration procedure with bioresorbable membranes versus conventional flap surgery in the treatment of infrabony periodontal defects, J. Clin. Periodontol. 27 (2000) 120–127.
[4] L. Hammarström, Enamel matrix, cementum development and regeneration, J. Clin. Periodontol. 24 (1997) 658–668.
[5] I. Darby, Periodontal materials, Aust. Dent J. 56 (2011) 107–118.
[6] B.L. Eppley, W.S. Pietrzak, M. Blanton, Allograft and alloplastic bone substitutes: a review of science and technology for the craniomaxillofacial surgeon, J. Craniofac. Surg. 16 (2005) 981–989.
[7] R. Langer, J.P. Vacanti, Tissue engineering, Science 260 (1993) 920–926.
[8] L. Chen, E.E. Tredget, P.Y. Wu, Y. Wu, Paracrine factors of mesenchymal stem cells recruit macrophages and endothelial lineage cells and enhance wound healing, PLoS One 3 (2008) e1886.
[9] P.R. Baraniak, T.C. McDevitt, Stem cell paracrine actions and tissue regeneration, Regen. Med. 5 (2010) 121–143.
[10] M. Gnecchi, H. He, O.D. Liang, L.G. Melo, F. Morello, H. Mu, N. Noiseux, L. Zhang, R.E. Pratt, J.S. Ingwall, V.J. Dzau, Paracrine action accounts for marked protection of ischemic heart by Akt-modified mesenchymal stem cells, Nat. Med. 11 (2005) 367–368.
[11] T. Kinnaird, E. Stabile, M.S. Burnett, M. Shou, C.W. Lee, S. Barr, S. Fuchs, S.E. Epstein, Local delivery of marrow-derived stromal cells augments collateral perfusion through paracrine mechanisms, Circulation 109 (2004) 1543–1549.
[12] M. Osugi, W. Katagiri, R. Yoshimi, T. Inukai, H. Hibi, M. Ueda, Conditioned media from mesenchymal stem cells enhanced bone regeneration in rat calvarial bone defects, Tissue Eng. Part A 23 (2012) 1479–1489.
[13] S. Kadiyala, R.G. Young, M.A. Thiede, S.P. Bruder, Culture expanded canine mesenchymal stem cells possess osteochondrogenic potential in vivo and in vitro, Cell Transplant. 6 (1997) 125–134.
[14] T. Nakahara, T. Nakamura, E. Kobayashi, K. Kuremoto, T. Matsuno, Y. Tabata, K. Eto, Y. Shimizu, In situ tissue engineering of periodontal tissues by seeding with periodontal ligament-derived cells, Tissue Eng. 10 (2004) 537–544.
[15] C.S. Kim, S.H. Choi, K.S. Cho, J.K. Chai, U.M. Wikesjö, C.K. Kim, Periodontal healing in one-wall intra-bony defects in dogs following implantation of autogenous bone or a coral-derived biomaterial, J. Clin. Periodontol. 32 (2005) 583–589.
[16] L.T. Kurz, S.R. Garfin, R.E. Booth Jr, Harvesting autogenous iliac bone grafts. A review of complications and techniques, Spine 14 (1989) 1324–1331.
[17] M.R. Dragoo, H.C. Sullivan, A clinical and histological evaluation of autogenous iliac bone grafts in humans. II. External root resorption, J. Periodontol. 44 (1973) 614–625.
[18] X.E. Dereka, C.E. Markopoulou, I.A. Vrotsos, Role of growth factors on periodontal repair, Growth Factors 24 (2006) 260–267.
[19] G. Pellegrini, Y.J. Seol, R. Gruber, W.V. Giannobile, Pre-clinical models for oral and periodontal reconstructive therapies, J. Dent. Res. 88 (2009) 1065–1076.
[20] M. Kitamura, K. Nakashima, Y. Kowashi, T. Fujii, H. Shimauchi, T. Sasano, T. Furuuchi, M. Fukuda, T. Noguchi, T. Shibutani, Y. Iwayama, S. Takashiba, H. Kurihara, M. Ninomiya, J. Kido, T. Nagata, T. Hamachi, K. Maeda, Y. Hara, Y. Izumi, T. Hirofuji, E. Imai, M. Omae, M. Watanuki, S. Murakami, Periodontal tissue regeneration using fibroblast growth factor-2: randomized controlled phase II clinical trial, PLoS ONE 3 (2008) e2611.
[21] S. Mohammed, A.R. Pack, T.B. Kardos, The effect of transforming growth factor beta one (TGF-beta 1) on wound healing, with or without barrier membranes, in a Class II furcation defect in sheep, J. Periodont. Res. 33 (1998) 335–344.
[22] W.V. Giannobile, S. Ryan, M.S. Shih, D.L. Su, P.L. Kaplan, T.C. Chan, Recombinant human osteogenic protein-1 (OP-1) stimulates periodontal wound healing in class III furcation defects, J. Periodontol. 69 (1998) 129–137.
[23] K. Takeda, H. Shiba, N. Mizuno, N. Hasegawa, Y. Mouri, A. Hirachi, H. Yoshino, H. Kawaguchi, H. Kurihara, Brain-derived neurotrophic factor enhances periodontal tissue regeneration, Tissue Eng. 11 (2005) 1618–1629.
[24] T.G. Kim, U.M. Wikesjö, K.S. Cho, J.K. Chai, S.D. Pippig, M. Siedler, C.K. Kim, Periodontal wound healing/regeneration following implantation of recombinant human growth/differentiation factor-5 (rhGDF-5) in an absorbable collagen sponge carrier into one-wall intrabony defects in dogs: a dose-range study, J. Clin. Periodontol. 36 (2009) 589–597.
[25] H.R. Kwon, U.M. Wikesjö, J.C. Park, Y.T. Kim, P. Bastone, S.D. Pippig, C.K. Kim, Growth/differentiation factor-5 significantly enhances periodontal wound healing/regeneration compared with platelet-derived growth factor-BB in dogs, J. Clin. Periodontol. 37 (2010) 739–746.
[26] C.K. Min, U.M. Wikesjö, J.C. Park, G.J. Chae, S.D. Pippig, P. Bastone, C.S. Kim, C.K. Kim, Wound healing/regeneration using recombinant human growth / differentiation factor-5 in an injectable poly-lactide-co-glycolide-acid composite carrier and a one-wall intra-bony defect model in dogs, J. Clin. Periodontol. 38 (2011) 261–268.
[27] D. Kaigler, J.A. Cirelli, W.V. Giannobile, Growth factor delivery for oral and periodontal tissue engineering, Expert Opin. Drug Deliv. 3 (2006) 647–662.
[28] K. Kawasaki, M. Aihara, J. Honmo, S. Sakurai, Y. Fujimaki, K. Sakamoto, E. Fujimaki, J.M. Wozney, A. Yamaguchi, Effects of recombinant human bone morphogenetic protein-2 on differentiation of cells isolated from human bone, muscle, and skin, Bone 23 (1998) 223–231.
[29] B. Perri, M. Cooper, C. Lauryssen, N. Anand, Adverse swelling associated with use of rh-BMP-2 in anterior cervical discectomy and fusion: a case study, Spine J. 7 (2007) 235–239.
[30] Z.S. Patel, S. Young, Y. Tabata, J.A. Jansen, M.E. Wong, A.G. Mikos, Dual delivery of an angiogenic and an osteogenic growth factor for bone regeneration in a critical size defect model, Bone 43 (2008) 931–940.
[31] F.M. Chen, R. Chen, X.J. Wang, H.H. Sun, Z.F. Wu, In vitro cellular responses to scaffolds containing two microencapsulated growth factors, Biomaterials 30 (2009) 5215–5224.
[32] D.H. Kempen, L. Lu, A. Heijink, T.E. Hefferan, L.B. Creemers, A. Maran, M.J. Yaszemski, W.J. Dhert, Effect of local sequential VEGF and BMP-2 delivery on ectopic and orthotopic bone regeneration, Biomaterials 30 (2009) 2816–2825.
[33] F.M. Chen, Y. An, R. Zhang, M. Zhang, New insights into and novel applications of release technology for periodontal reconstructive therapies, J. Control Release 149 (2011) 92–110.
[34] K. Okuda, K. Yamamiya, T. Kawase, H. Mizuno, M. Ueda, H. Yoshie, Treatment of human infrabony periodontal defects by grafting human cultured periosteum sheets combined with platelet-rich plasma and porous hydroxyapatite granules: case series, J. Int. Acad. Periodontol. 11 (2009) 206–213.
[35] Y. Yamada, M. Ueda, T. Naiki, M. Takahashi, K. Hata, T. Nagasaka, Autogenous injectable bone for regeneration with mesenchymal stem cells and platelet-rich plasma: tissue-engineered bone regeneration, Tissue Eng. 10 (2004) 955–964.
[36] J. Müller-Ehmsen, P. Whittaker, R.A. Kloner, J.S. Dow, T. Sakoda, T.I. Long, P.W. Laird, L. Kedes, Survival and development of neonatal rat cardiomyocytes transplanted into adult myocardium, J. Mol. Cell Cardiol. 34 (2002) 107–116.

[37] H. Reinecke, C.E. Murry, Transmural replacement of myocardium after skeletal myoblast grafting into the heart. Too much of a good thing?, Cardiovasc Pathol. 9 (2000) 337–344.
[38] M. Zhang, D. Methot, V. Poppa, Y. Fujio, K. Walsh, C.E. Murry, Cardiomyocyte grafting for cardiac repair: graft cell death and anti-death strategies, J. Mol. Cell Cardiol. 33 (2001) 907–921.
[39] H. Reinecke, C.E. Murry, Taking the death toll after cardiomyocyte grafting: a reminder of the importance of quantitative biology, J. Mol. Cell Cardiol. 34 (2002) 251–253.
[40] C. Ide, Y. Nakai, N. Nakano, T.B. Seo, Y. Yamada, K. Endo, T. Noda, F. Saito, Y. Suzuki, M. Fukushima, T. Nakatani, Bone marrow stromal cell transplantation for treatment of sub-acute spinal cord injury in the rat, Brain Res. 1332 (2010) 32–47.
[41] N. Nakano, Y. Nakai, T.B. Seo, Y. Yamada, T. Ohno, A. Yamanaka, Y. Nagai, M. Fukushima, Y. Suzuki, T. Nakatani, C. Ide, Characterization of conditioned medium of cultured bone marrow stromal cells, Neurosci. Lett. 483 (2010) 57–61.
[42] J. Cornish, A. Grey, K.E. Callon, D. Naot, B.L. Hill, C.Q. Lin, L.M. Balchin, I.R. Reid, Shared pathways of osteoblast mitogenesis induced by amylin, adrenomedullin, and IGF-1, Biochem. Biophys. Res. Commun. 318 (2004) 240–246.
[43] Y. Li, X. Yu, S. Lin, X. Li, S. Zhang, Y.H. Song, Insulin-like growth factor 1 enhances the migratory capacity of mesenchymal stem cells, Biochem. Biophys. Res. Commun. 356 (2007) 780–784.
[44] X. Han, S. Amar, Role of insulin-like growth factor-1 signaling in dental fibroblast apoptosis, J. Periodontol. 74 (2003) 1176–1182.
[45] D. Kaigler, P.H. Krebsbach, P.J. Polverini, D.J. Mooney, Role of vascular endothelial growth factor in bone marrow stromal cell modulation of endothelial cells, Tissue Eng. 9 (2003) 95–103.
[46] K. Janssens, P. ten Dijke, S. Janssens, W. Van Hul, Transforming growth factor-beta1 to the bone, Endocr. Rev. 26 (2005) 743–774.
[47] T. Fujita, H. Shiba, T.E. Van Dyke, H. Kurihara, Differential effects of growth factors and cytokines on the synthesis of SPARC, DNA, fibronectin and alkaline phosphatase activity in human periodontal ligament cells, Cell Biol. Int. 28 (2004) 281–286.
[48] J. Gao, A.L. Symons, P.M. Bartold, Expression of transforming growth factor-beta 1 (TGF-beta1) in the developing periodontium of rats, J. Dent. Res. 77 (1998) 1708–1716.
[49] Y. Taniyama, R. Morishita, K. Hiraoka, M. Aoki, H. Nakagami, K. Yamasaki, K. Matsumoto, T. Nakamura, Y. Kaneda, T. Ogihara, Therapeutic angiogenesis induced by human hepatocyte growth factor gene in rat diabetic hind limb ischemia model: molecular mechanisms of delayed angiogenesis in diabetes, Circulation 104 (2001) 2344–2350.
[50] R. Matsui, Development of TERUDERMIS, collagen-based artificial dermis and TERUPLUG, collagen-based material for extraction sockets, J. Jpn. Assoc. Regenerative Dent. 6 (2008) 9–20.

Human Dental Pulp-Derived Stem Cells Protect Against Hypoxic-Ischemic Brain Injury in Neonatal Mice

Mari Yamagata, DDS; Akihito Yamamoto, DDS, PhD; Eisuke Kako, MD, PhD; Naoko Kaneko, MD, PhD; Kohki Matsubara, DDS; Kiyoshi Sakai, DDS, PhD; Kazunobu Sawamoto, PhD; Minoru Ueda, DDS, PhD

Background and Purpose—Perinatal hypoxia-ischemia (HI) has high rates of neurological deficits and mortality. So far, no effective treatment for HI brain injury has been developed. In this study, we investigated the therapeutic effects of stem cells from human exfoliated deciduous teeth (SHED) for the treatment of neonatal HI brain injury.

Methods—Unilateral HI was induced in postnatal day 5 (P5) mice. Twenty-four hours later, SHED, human skin fibroblasts, or serum-free conditioned medium derived from these cells was injected into the injured brain. The effects of cell transplantation or conditioned medium injection on the animals' neurological and pathophysiological recovery were evaluated.

Results—Transplanted SHED, but not fibroblasts, significantly reduced the HI-induced brain-tissue loss and improved neurological function. SHED also improved the survival of the HI mice. The engrafted SHED rarely differentiated into neural lineages; however, their transplantation inhibited the expression of proinflammatory cytokines, increased the expression of anti-inflammatory ones, and significantly reduced apoptosis. Notably, the intracerebral administration of SHED-conditioned medium also significantly improved the neurological outcome, inhibited apoptosis, and reduced tissue loss.

Conclusions—SHED transplantation into the HI-injured brain resulted in remarkable neurological and pathophysiological recovery. Our findings indicate that paracrine factors derived from SHED support a neuroprotective microenvironment in the HI brain. SHED graft and SHED-conditioned medium may provide a novel neuroprotective therapy for HI. **(*Stroke*. 2013;44:551-554.)**

Key Words: cell transplantation ■ functional recovery ■ inflammation ■ neonatal ischemia ■ stem cells ■ trophic factors

Stem cells from human exfoliated deciduous teeth (SHED) reside within the perivascular niche of the dental pulp. They are thought to originate from the cranial neural crest, and express early markers for both mesenchymal and neuroectodermal stem cells.[1,2] We previously showed that SHED transplantation into the completely transected rat spinal cord results in remarkable functional recovery of hindlimb locomotion.[2] However, whether engrafted SHED or the paracrine factors derived from them can offer therapeutic benefits in other neurological disease settings is still largely unknown. In this study, we investigated the therapeutic benefits of SHED on mouse neonatal hypoxia-ischemia (HI).

Materials and Methods

An expanded version of the Methods section is available in the online-only Data Supplement. SHED, human skin fibroblasts, and their serum-free conditioned medium (CM) were prepared as described.[2] The SHED's multi-differentiation potential and their expression of both mesenchymal stem cell and neural lineage markers were similar to those reported previously.[2] HI brain injury was induced in postnatal day 5 (P5) mice as described. Cells (2×10^5) in 2 μL phosphate buffered saline or phosphate buffered saline alone (as a control) were transplanted into the ipsilateral hemisphere at 2.0 mm anterior and 2.0 mm lateral to bregma, and 2.0 mm deep to the dural surface, using a glass needle and a Kopf microstereotaxic injection system, 24 hours after HI (Figure 1A). These animals were given daily administration of cyclosporin A (Novartis, Nurnberg, Germany, 10 mg/kg, IP) throughout the experimental period, except when they were used for cytokine expression analysis. For the experiments using CM, mice were given a 2-μL injection of CM or Dulbecco's modification of Eagle's medium (as a control) without cyclosporin A treatment. The animals' neurological recovery was examined by a foot-fault test in 4-, 6-, and 8-week-old HI mice.[3] Tissue loss was examined by staining with hematoxylin and eosin, and brain injury was evaluated using a neuropathological scoring system,[4,5] by an observer blinded to the identity of the animal group. The level of apoptosis was analyzed by staining with anticaspase-3 (Cell Signaling). Real-time reverse transcription PCR was carried out as described.[2] GAPDH cDNA was amplified as an internal control. Primer sequences are shown in the online-only Supplemental Table 1.

Data are expressed as means±SEM. Survival data were analyzed by applying the Kaplan-Meier curve, followed by the Mental-Cox

Received September 12, 2012; final revision received October 12, 2012; accepted October 19, 2012.

From the Department of Oral and Maxillofacial Surgery, Nagoya University Graduate School of Medicine, Nagoya, Japan (M.Y., A.Y., K.M., K.S., M.U.); and Department of Developmental and Regenerative Biology (M.Y., E.K., N.K., K.S.), and Anesthesiology and Medical Crisis Management (E.K.), Nagoya City University Graduate School of Medical Sciences, Nagoya, Japan.

The online-only Data Supplement is available with this article at http://stroke.ahajournals.org/lookup/suppl/doi:10.1161/STROKEAHA.112.676759/-/DC1.

Correspondence to Akihito Yamamoto, Nagoya University Graduate School of Medicine, 65 Tsurumai-cho, Showa-ku, Nagoya 466-8550, Japan. E-mail akihito@med.nagoya-u.ac.jp

***Stroke* is available at http://stroke.ahajournals.org** **DOI: 10.1161/STROKEAHA.112.676759**

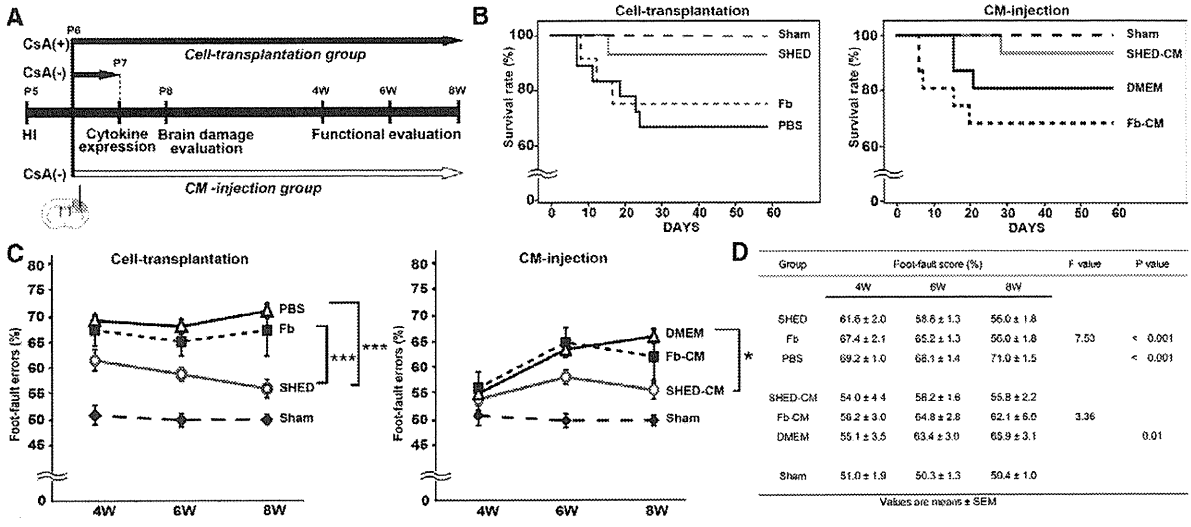

Figure 1. Neurological outcomes and survival rate after HI. **A**, Experimental protocol. Mice underwent HI insult at P5, and then received cell transplantation (Cell) or CM injection (CM) at P6. In the analyses of cell transplantation's effects on functional recovery and brain damage, the phosphate buffered saline-, Fb-, and SHED-treated groups received daily administrations of cyclosporin A (CsA). The cytokine assay and brain damage evaluation were performed at P7 and P8, respectively. Neurological recovery was examined at 4, 6, and 8 weeks. **B**, Survival curve (SHED n =14; Fb n=12; PBS n = 18; SHED-CM n = 16; Fb-CM n = 16; DMEM n = 16; Sham n = 5). **C**, Foot-fault test (SHED n=12; Fb n=9; PBS n = 9; SHED-CM n = 15; Fb-CM n = 10; DMEM n = 13; Sham n = 5). **D**, Statistic data. Values are means±SEM, $^{*}P< 0.05$, $^{***}P< 0.001$.

log-rank test to identify differences between the curves. Behavioral data were analyzed by 2-way ANOVA. Comparisons of parameters among the groups were made by 1-way ANOVA. Post-hoc analyses were performed with Bonferroni test. All statistical analyses were performed with Stata version 11.0 (Stata Corp, College Station, TX). A value of $P<0.05$ was considered statistically significant.

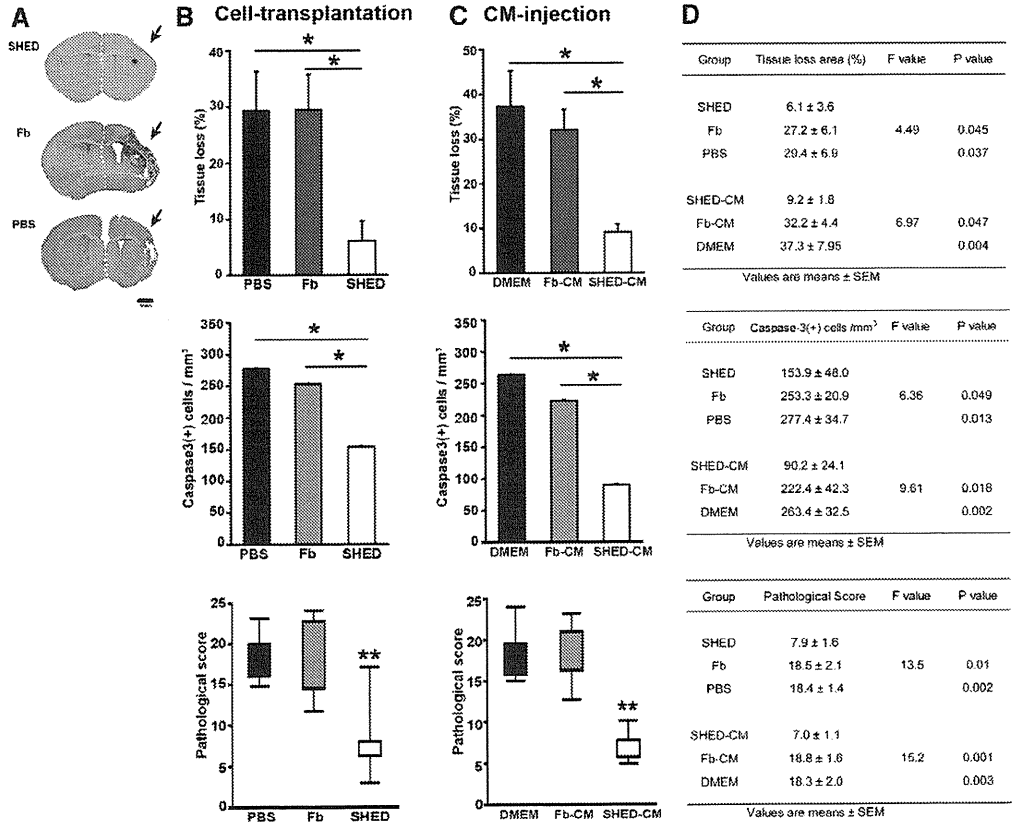

Figure 2. Histological evaluation. **A**, Representative HE-stained coronal brain sections. Scale bar: 1 mm. **B**, Cell-transplantation. **C**, Conditioned medium (CM)-injection. Tissue loss (each group, n=10–12); Caspase-3 (+) cells (each group, n=6); Pathological score (each group, n=5–8). **D**, Statistic data. Values are means±SEM, n=6 per group, $^{*}P<0.05$, $^{**}P<0.01$.

Results

The HI mice that underwent SHED transplantation exhibited significant neurological recovery compared with the fibroblasts- and phosphate buffered saline-treated groups (Figure 1C). The SHED-transplanted group also displayed better survival over time (Figure 1B). Histological examination revealed that the tissue loss, number of apoptotic cells, and neuropathological score in the SHED-transplanted group were significantly lower than in the other experimental groups (Figure 2A and B). Cell-type analysis showed that the apoptosis of neurons in the cortex, corpus callosum, and hippocampus and of oligodendrocytes in the corpus callosum was significantly reduced in the SHED-transplanted group (online-only Supplemental Figure 2).

The expression levels of proinflammatory cytokines interleukin-1β and tumor necrosis factor-α were upregulated in the phosphate buffered saline- and fibroblasts-transplanted groups 24 hours after HI, but those of anti-inflammatory cytokines interleukin-4 and interleukin-10 were downregulated. Notably, engrafted SHED significantly suppressed the expression of proinflammatory cytokines, whereas strongly upregulating anti-inflammatory cytokines (Figure 3).

Eight weeks after transplantation, little or no SHED had differentiated into neurons, oligodendrocytes, or astrocytes (online-only Supplemental Figure 3). Taken together, these results suggested that SHED promoted recovery after HI by paracrine mechanisms. In support of this idea, we found that mice receiving a 2-μL injection of SHED-CM in the HI-injured brain exhibited significant or better recovery in neurological function (Figure 1C), survival rate (Figure 1B), and neuropathological score (Figure 2C) than those receiving fibroblasts-CM or cell-culture medium (Dulbecco's modification of Eagle's medium) alone.

Discussion

Here we demonstrated that the transplantation of SHED into the HI-injured mouse brain improved the neurological outcome and survival rate. The engrafted SHED shifted the HI-induced proinflammatory state to an anti-inflammatory one and inhibited apoptosis and tissue loss. Importantly, mice receiving an injection of 2 μL SHED-CM 24 hours after HI exhibited significant recovery as assessed by both neurological and pathological examinations. These results suggest that most of the SHED-mediated therapeutic benefits were elicited by paracrine mechanisms. It was difficult to compare the level of therapeutic benefits between engrafted SHED and SHED-CM, because in the SHED experiments, the administration of cyclosporin A, which protects engrafted cells from the xenogeneic host immune response, significantly suppressed the HI-induced inflammatory response and apoptosis[6] (online-only Supplemental Figure 4). Furthermore, cell transplantation may have an advantage in providing a prolonged delivery of paracrine factors, compared with the transient delivery by the CM treatment.

Previous reports indicate that the engraftment of various types of transplanted stem cells is a promising regenerative therapy for HI.[7] However, for clinical use, mesenchymal stem cells must be expanded by a reliable cell-culture system that produces sufficient cell numbers to elicit clinical benefits, while also meeting safety requirements. These severe restrictions may impede the progress of regenerative therapy for HI. Our data suggest that the administration of SHED-CM provides a portion of the therapeutic benefit of SHED

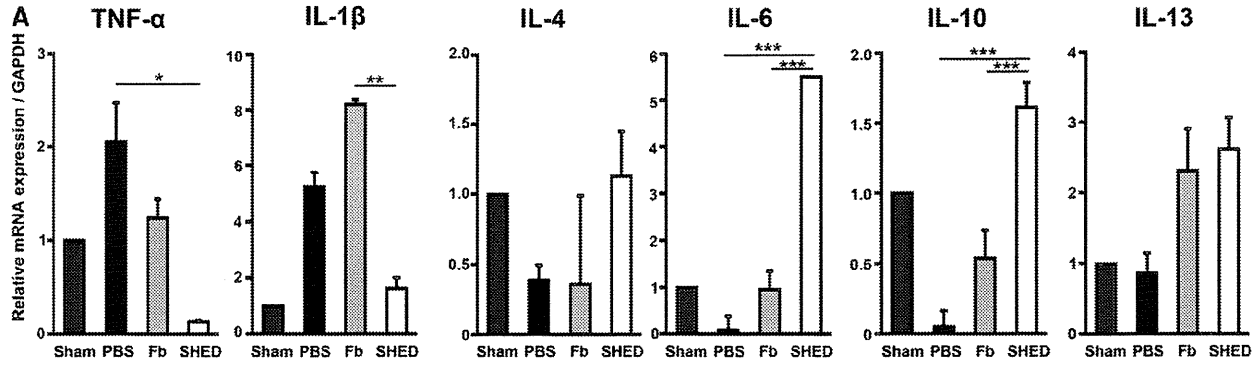

B

Primer	Relative mRNA expression / GAPDH			F value	P value
	SHED	Fb	PBS		
TNF-α	0.13 ± 0.0	1.24 ± 0.2	2.05 ± 0.5	3.7	0.04
IL-1β	1.62 ± 0.2	6.18 ± 0.2	5.23 ± 0.3	6.34	0.007
IL-4	1.12 ± 0.6	0.36 ± 0.1	0.39 ± 0.1		
IL-6	5.50 ± 0.4	0.95 ± 0.3	0.08 ± 0.0	36.8	< 0.001
IL-10	1.61 ± 0.2	0.53 ± 0.1	0.05 ± 0.0	30.3	< 0.001
IL-13	2.61 ± 0.6	2.30 ± 0.3	0.86 ± 0.3		

Values are means ± SEM

Figure 3. **A**, Quantitative real-time reverse transcription polymerase chain reaction analysis in cell-transplantation groups. Relative mRNA expression of tumor necrosis factor-α, interleukin (IL)-1β, IL-4, IL-6, IL-10, and IL-13 compared with that in sham-operated mice. **B**, Statistic data. Values are means±SEM. *P<0.05, **P<0.01, ***P<0.001.

transplantation, and this finding may be useful in establishing a practical regeneration therapy for HI.

Acknowledgments

We thank the Division of Experimental Animals and Medical Research Engineering, Nagoya City University Graduate School of Medical Sciences, for housing the mice and for microscope maintenance.

Sources of Funding

This work was supported by Grants-in-Aid for Scientific Research on Priority Areas from the Ministry of Education, Culture, Sports, Science and Technology of Japan, Grants-in-Aid for the Practical Application of Regenerative Medicine from the Ministry of Health, Labor and Welfare of Japan, the Funding Program for Next Generation World-Leading Researchers (Japan Society for the Promotion of Science), and a Grant for COE for Education and Research of Micro-Nano Mechatronics of the Nagoya University Global COE Program.

Disclosures

None.

References

1. Miura M, Gronthos S, Zhao M, Lu B, Fisher LW, Robey PG, et al. SHED: stem cells from human exfoliated deciduous teeth. *Proc Natl Acad Sci USA*. 2003;100:5807–5812.
2. Sakai K, Yamamoto A, Matsubara K, Nakamura S, Naruse M, Yamagata M, et al. Human dental pulp-derived stem cells promote locomotor recovery after complete transection of the rat spinal cord by multiple neuro-regenerative mechanisms. *J Clin Invest*. 2012;122:80–90.
3. Kako E, Kaneko N, Aoyama M, Hida H, Takebayashi H, Ikenaka K, et al. Subventricular zone-derived oligodendrogenesis in injured neonatal white matter in mice enhanced by a nonerythropoietic erythropoietin derivative. *Stem Cells*. 2012;30:2234–2247.
4. Cheng Y, Gidday JM, Yan Q, Shah AR, Holtzman DM. Marked age-dependent neuroprotection by brain-derived neurotrophic factor against neonatal hypoxic-ischemic brain injury. *Ann Neurol*. 1997;41:521–529.
5. Thoresen M, Bågenholm R, Løberg EM, Apricena F, Kjellmer I. Posthypoxic cooling of neonatal rats provides protection against brain injury. *Arch Dis Child Fetal Neonatal Ed*. 1996;74:F3–F9.
6. Hwang JH, Lee JH, Lee KH, Bae EJ, Sung DK, Chang YS, et al. Cyclosporine A attenuates hypoxic-ischemic brain injury in newborn rats. *Brain Res*. 2010;1359:208–215.
7. Bennet L, Tan S, Van den Heuij L, Derrick M, Groenendaal F, van Bel F, et al. Cell therapy for neonatal hypoxia-ischemia and cerebral palsy. *Ann Neurol*. 2012;71:589–600.